Accelerated Formation of Cubic Phases in Phosphatidylethanolamine Dispersions

Boris Tenchov,* Rumiana Koynova,* and Gert Rapp#
*Institute of Biophysics, Bulgarian Academy of Sciences, 1113 Sofia, Bulgaria, and #European Molecular Biology Laboratory Outstation at Deutsches Elektronen-Synchrotron, D-22603 Hamburg, Germany

ABSTRACT By means of x-ray diffraction we show that several sodium salts and the disaccharides sucrose and trehalose strongly accelerate the formation of cubic phases in phosphatidylethanolamine (PE) dispersions upon temperature cycling through the lamellar liquid crystalline–inverted hexagonal (L_α-H_{II}) phase transition. Ethylene glycol does not have such an effect. The degree of acceleration increases with the solute concentration. Such an acceleration has been observed for dielaidoyl PE (DEPE), dihexadecyl PE, and dipalmitoyl PE. It was investigated in detail for DEPE dispersions. For DEPE (10 wt% of lipid) aqueous dispersions at 1 M solute concentration, 10–50 temperature cycles typically result in complete conversion of the L_α phase into cubic phase. Most efficient is temperature cycling executed by laser flash T-jumps. In that case the conversion completes within 10–15 cycles. However, the cubic phases produced by laser T-jumps are less ordered in comparison to the rather regular cubic structures produced by linear, uniform temperature cycling at 10°C/min. Temperature cycles at scan rates of 1–3°C/min also induce the rapid formation of cubic phases. All solutes used induce the formation of Im3m (Q^{229}) cubic phase in 10 wt% DEPE dispersions. The initial Im3m phases appearing during the first temperature cycles have larger lattice parameters that relax to smaller values with continuation of the cycling after the disappearance of the L_α phase. A cooperative Im3m → Pn3m transition takes place at ~85°C and transforms the Im3m phase into a mixture of coexisting Pn3m (Q^{224}) and Im3m phases. The Im3m/Pn3m lattice parameter ratio is 1.28, as could be expected from a representation of the Im3m and Pn3m phases with the primitive and diamond infinite periodic minimal surfaces, respectively. At higher DEPE contents (~30 wt%), cubic phase formation is hindered after 20–30 temperature cycles. The conversion does not go through, but reaches a stage with coexisting Ia3d (Q^{230}) and L_α phases. Upon heating, the Ia3d phase cooperatively transforms into a mixture of, presumably, Im3m and Pn3m phases at about the temperature of the L_α-H_{II} transition. This transformation is readily reversible with the temperature. The lattice parameters of the DEPE cubic phases are temperature-insensitive in the L_α temperature range and decrease with the temperature in the range of the H_{II} phase.

INTRODUCTION

The ability of various surfactants, membrane lipids, and their mixtures with other compounds to form cubic phases in aqueous dispersions has been known for long time (Luzzati, 1968). Over that time, numerous investigations of the properties of these phases have been carried out. A number of review articles summarize the advancements in this field (see, e.g., Mariani et al., 1988; Lindblom and Rilfors, 1989; Fontell, 1990; Seddon, 1990; Seddon and Templer, 1993, 1995; Luzzati et al., 1993, 1996, 1997). Seven different cubic phases with space groups Q^{212}, Q^{223}, Q^{224}, Q^{225}, Q^{227}, Q^{229}, Q^{230} have been identified so far (Luzzati et al., 1996, 1997). Various proposals referring to the biological role of the nonlamellar lipid patterns have been published (see, e.g., Luzzati, 1997, for an overview). It is believed that such patterns are a part of the processes of cell fusion, transport and secretion of macromolecules across membranes, cell-cell and cell-virus interactions, fat digestion, membrane repair, and cell damage caused by extreme conditions. Evidence for the role of nonlamellar lipids in maintaining the functional state of integral membrane proteins has recently been accumulated (Rietveld et al., 1995; Bogdanov et al., 1996; de Kruijff, 1997). It has been argued that the lipid metabolism regulatory mechanisms maintain the membrane lipid composition in the vicinity of a lamellar-isotropic (cubic) transition, so that a conversion into the nonlamellar phase can easily be triggered by small perturbations (Lindblom and Rilfors, 1989, 1990). The geometric description of some of the cubic phases with infinite periodic minimal surfaces has provided new hints of a possible physiological significance of the bilayer transitions from planar into cubic geometry (Larsson, 1988, 1989). Morphological analysis suggests that membranous cellular structures such as, for example, the rough endoplasmic reticulum, are best described as cubic structures and that these structures might serve as subcellular space organizers (Landh, 1995).

In addition to the spontaneously forming cubic phases, a cubic phase may also appear as a result of extensive temperature cycling through the $L_\alpha \leftrightarrow H_{II}$ phase transition of a lipid/water system. The 1,2-dioleoyl-*sn*-glycero-3-phosphoethanolamine/water (DOPE/water) system represents an example of such behavior. Cycling through its $L_\alpha \leftrightarrow H_{II}$ transition several hundred or thousand times converts this system from L_α to cubic phase (Shyamsunder et al., 1988; Erbes et al., 1994). The number of cycles required shows that a small fraction of the lipid, of the order of 0.1%,

Received for publication 30 December 1997 and in final form 5 May 1998.
Address reprint requests to Dr. Boris Tenchov, Institute of Biophysics, Bulgarian Academy of Sciences, Acad. G. Bonchev str., block 21, 1113 Sofia, Bulgaria. Tel. 359-2-9713969; Fax: 359-2-9712493; E-mail: tenchov@obzor.bio21.acad.bg.

0006-3495/98/08/853/14 $2.00

rearranges from lamellar into cubic structure during each cycle. The resistance of the lipid to such rearrangement is thought to be associated with a large kinetic barrier imposed by the different geometries of the two phases. It is therefore of interest to define conditions that would influence the conversion rate and eventually accelerate the formation of cubic phases.

In a study of disaccharide effects on the phase behavior of saturated PEs, we noticed that DPPE and DHPE dispersed in sucrose solutions partially convert to cubic phase when cooled from the H_{II} to the L_α phase (Tenchov et al., 1996). This observation led us to expect that a small number of temperature cycles would be sufficient for complete transformation of these dispersions into cubic phase. In the present work we investigated this possibility and found that, along with the disaccharides, the sodium salts also strongly promote the formation of cubic phases in PEs during temperature cycling. The acceleration effect was demonstrated for several PEs that do not spontaneously form such phases in excess water. It was studied in detail for DEPE dispersions. The measurements were carried out by time-resolved x-ray diffraction. Because the temperature cycling was directly executed on samples mounted on the beam line, it was possible to follow in real time the conversion from lamellar to cubic phase.

MATERIALS AND METHODS

Sample preparation

1,2-Dielaidoyl-sn-glycero-3-phosphoethanolamine (DEPE) and 1,2-dipalmitoyl-*sn*-glycero-3-phosphoethanolamine (DPPE) were purchased from Avanti Polar Lipids (Birmingham, AL); 1,2-dihexadecyl-sn-glycero-3-phosphoethanolamine (DHPE) was purchased from Fluka AG (Buchs, Switzerland). All lipids were found to migrate as a single spot in thin-layer chromatography checks. Microcalorimetric scans of their diluted dispersions showed highly cooperative phase transitions at temperatures in agreement with the published values. Sodium salts NaH_2PO_4, Na_2SO_4, and NaCl (Merck); NaSCN (Sigma); sucrose (Sigma); trehalose (Fluka); ethyleneglycol (Sigma); and bidistilled deionized water were used.

Samples with 10 wt% lipid concentration were prepared by dispersing a weighed amount of lipid into the required amount of the appropriate solution. The dispersions were homogenized by cycling 8–10 times between 75°C and an ice bath and vortex-mixed at these temperatures for 1–2 min. Samples of higher lipid concentration were prepared by dispersing weighed a amount of lipid into the appropriate solution to a lipid concentration 3–5 wt%. The dispersions were homogenized by the above procedure and centrifuged at 14,000 rpm for 30 min with a benchtop centrifuge. The free solution was removed with a syringe, and the lipid pellet was used for measurements. The final lipid concentration in these preparations, determined by weight, was within 25–35 wt% for dispersions in 1 M Na_2SO_4, NaH_2PO_4, NaCl, and NaSCN solutions. Later in the text we refer to these preparations as "30 wt% lipid dispersions." The lipid dispersions were sealed in glass capillaries, or in flat cells of 0.6 and 1 mm thickness, and stored at room temperature for several hours to 1–2 days before the measurement.

X-ray measurements

X-ray diffraction patterns were recorded on beam line X13 of the EMBL outstation at Deutsches Elektronen-Synchrotron (DESY), Hamburg. The camera geometry and the data acquisition system were as described in detail previously (Rappolt and Rapp, 1996). To achieve better resolution, most of the measurements were made with a single linear detector (Gabriel, 1977) placed ~330 cm from the sample. It covers the small-angle region from 1/(65 nm) to about 1/(2.5 nm) with a resolution of $1/\Delta s = 5.94 \times 10^{-4}$ nm. Occasional patterns recorded with a Fuji image plate system did not show angular dependence of the scattered intensity for the phases studied. Other setups with two detectors recording simultaneously from the small-angle and wide-angle regions (Rapp et al., 1995) were also used. Raw data were normalized for the incident beam intensity, and no other corrections were applied. Their analysis was carried out with the interactive data-evaluating program OTOKO (Boulin et al., 1986)

Temperature cycling

The temperature cycling was directly executed on samples mounted in the sample holder. Three cycling methods with different rates of temperature change were used:

1. Fast heating by laser flash T-jumps followed by relaxation of the sample temperature to the initial value. The setup used comprises a home-built erbium pulse laser equipped with a focusing system (Rapp and Goody, 1991). It deposits ~1 J of energy into the sample per single flash. The pulse duration was 2.5 ms. The laser spot at the sample position was 2–3 mm, with the incident x-ray beam focused at its center. The average magnitude of the T-jumps was 30–35°C, as determined from kinetic measurements on gel-liquid crystalline lipid phase transitions. The temperature relaxation times were measured with a thermocouple inserted into capillaries and flat cells filled with water and was found to be ~10–20 s. The initial temperature, T_{min}, was usually set at 10–15°C below the L_α-H_{II} phase transition and kept constant with a water bath.

2. Linear, uniform temperature cycling with a Peltier temperature control system at 10°C/min scan rate. The temperature cycles were typically programmed to start from a temperature T_{min} 15–20°C below the L_α-H_{II} phase transition. The heating step was immediately followed by a cooling step of the same rate and duration. The cooling step was usually followed by incubation for 1–2 min at T_{min} to ensure complete disappearance of the H_{II} phase. The cycle amplitudes varied in the range 20–60°C.

3. Temperature cycling with a PC-interfaced water bath with up to 3°C/min heating rate and 1.5°C/min cooling rate.

Radiation damage checks

We used two kinds of checks for potential artefacts due to lipid molecules damaged by radiation. The sample holder was mounted on a motorized stage. By moving it vertically and horizontally, it was possible to record and compare x-ray patterns from irradiated and several nonirradiated parts of the same sample. Although these patterns did not show radiation damage effects, such checks do not exclude, in principle, a possible influence of diffusion of degradation products into the nonirradiated sample parts. To eliminate completely the latter possibility, we implemented a simple but efficient method by using a two-capillary sample holder. Two capillaries containing the same sample were subjected to identical temperature treatment (temperature cycling) in the sample holder, but only one of them was irradiated in the course of the cycling, while the other capillary was kept in the dark. The sample holder was then moved to record x-ray patterns from the "dark" capillary. Such checks were carried out throughout all experiments. We detected no systematic differences between the x-ray patterns recorded from irradiated and nonirradiated capillaries and assume therefore that the results reported here were not affected by radiation damage of the lipid.

Phase behavior of DEPE, DHPE, and DPPE dispersions

Dispersions of DEPE, DHPE, and DPPE in excess water display reversible L_β-L_α transitions at 37°C, 69°C, and 62°C, respectively, and reversible L_α-H_{II} transitions at 64°C, 85°C, and 120°C, respectively (LIPIDAT

(http://www.lipidat.chemistry.ohio-state.edu); Koynova and Caffrey, 1994). Neither of these lipids is known to form cubic phase spontaneously. Their L_α phases are typified by sharp low-angle reflections and low levels of background scattering. No spontaneous disordering of the DEPE and DHPE lamellar phases takes place after incubation for several hours a few degrees below the L_α-H_{II} transition, in contrast to the behavior of monomethylated 1,2-dioleoyl-sn-glycero-3-phosphoethanolamine (m-DOPE) (Gagne et al., 1985; Gruner et al., 1988; Siegel and Banschbach, 1990). The sugars and the salts NaCl, Na_2SO_4, and NaH_2PO_4 increase the temperature of the phosphatidylethanolamine (PE) L_β-L_α transitions and depress their L_α-H_{II} transitions (for a summary, see Koynova et al., 1997a). The chaotropic salt NaSCN has the opposite effect. DEPE in 1 M NaSCN solution displays L_β-L_α transition at 35°C, and L_α-H_{II} transition at 85°C (Epand and Bryszewska, 1988).

RESULTS

In this work we demonstrate that several sodium salts (Na_2SO_4, NaH_2PO_4, NaCl, NaSCN) and the disaccharides sucrose and trehalose strongly accelerate the formation of cubic phases in DEPE, DPPE, and DHPE dispersions during temperature cycling through their L_α-H_{II} phase transitions. This effect was investigated in detail for DEPE dispersions. This lipid has L_β-L_α-H_{II} transitions at 37°C and 64°C, respectively. Thus it was possible to investigate the properties of the induced cubic phases upon deep heating into the H_{II} range, and to reset the system in the lamellar gel state merely by cooling to room temperature. Because of their higher L_α-H_{II} transition temperatures, DPPE and DHPE were less convenient to use with the present setup. For example, the L_α-H_{II} transition temperature of DPPE can be brought down to below 100°C only at rather high solute concentrations (Seddon et al., 1983; Tenchov et al., 1996; Koynova et al., 1997a). Still, it was also possible to record an acceleration effect for these lipids, with properties similar to those for DEPE.

Choice of temperature cycling method

Examples for the rapid evolution of the lipid structural organization in DEPE aqueous dispersions upon temperature cycling through the L_α-H_{II} transitions in the presence of different solutes are given in Figs. 1 and 2. A set of low-angle reflections that index on a cubic lattice progressively increase in intensity with the cycle number at the expense of the L_α first-order reflection. Most efficient was the temperature cycling executed by means of laser T-jumps. In that case, the conversion completes within 10–15 cycles (Fig. 1). It is limited to the sample portion under the laser spot. The cubic phases produced by laser T-jumps are less ordered compared to the rather regular cubic structures obtained by linear, uniform temperature cycling at 10°C/min (Fig. 2 and Fig. 3 *A* for DHPE). Their increased disorder might result from inhomogeneous sample heating. Temperature gradients arise not only at the boundary between the laser spot area and the rest of the sample, but possibly also within this area as a consequence of the lateral inhomogeneity (internal structure) of the laser beam. Temperature cycles at scan rates of 1–3°C/min also induce rapid formation of cubic phase in the presence of solutes (Fig. 3 *B*), in accord with our previous observations (Tenchov et al., 1996). However, such cycles are too slow to be followed for longer times. Thus we used a rate of 10°C/min as most appropriate for the induction of cubic phases. The cubic phases produced at such a cycling rate have well-resolved x-ray patterns, often with more than 10 low-angle reflections.

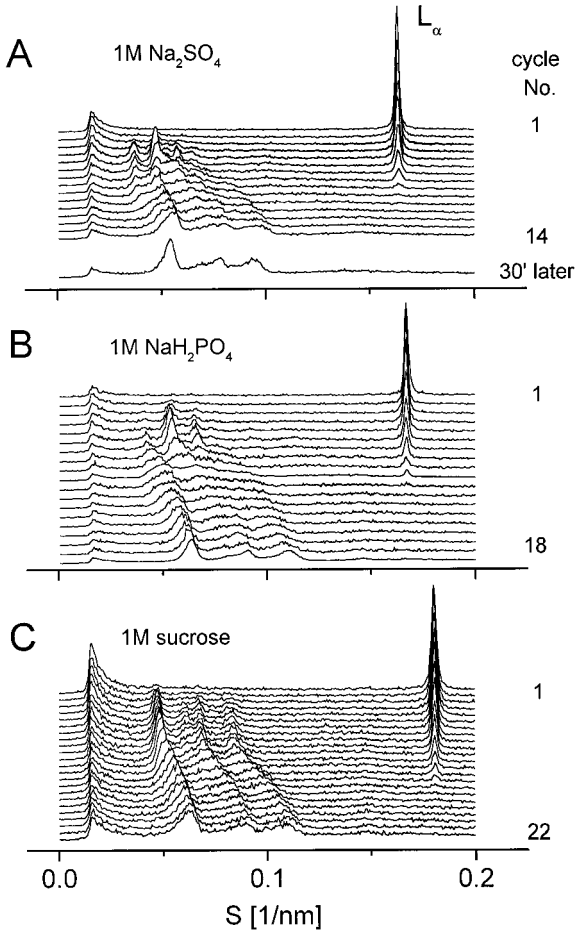

FIGURE 1 Conversion of 10 wt% DEPE dispersions in 1 M solutions from lamellar into cubic phase upon temperature cycling executed by laser-flash temperature jumps. The diffraction patterns shown were recorded immediately before the next T-jump. (*A*) 1 M Na_2SO_4, 47°C; sequence of 14 laser T-jumps executed from 47°C at 1-min intervals. Equilibration was followed for 30 min after the last T-jump. The phase assignment for the last frame recorded 30 min later is Im3m cubic phase (lattice parameter 26.2 nm) with an admixture of (possibly) Pn3m cubic phase. (*B*) 1 M NaH_2PO_4, 51°C; sequence of 18 laser T-jumps from 51°C at 3-min intervals. The assignment for the last frame recorded is Im3m phase (lattice parameter 22.4 nm) with an admixture of (possibly) Pn3m phase (Fig. 6 *A2*). (*C*) 1 M sucrose, 48°C; sequence of 22 laser T-jumps from 48°C at 3-min intervals. The T-jumps were followed by cooling to 41°C in 1 min, incubation for 1 min at 41°C, and heating back to 48°C in 1 min. The assignment for the last frame is Im3m phase, with a lattice parameter of 22.4 nm (Table 1).

With DEPE dispersions in Na_2SO_4, NaH_2PO_4, NaCl, and sucrose, the low end of the temperature cycle, T_{min}, was usually set at ~45–50°C. The maximum cycle temperature, T_{max}, was typically in the range 65–80°C, to ensure com-

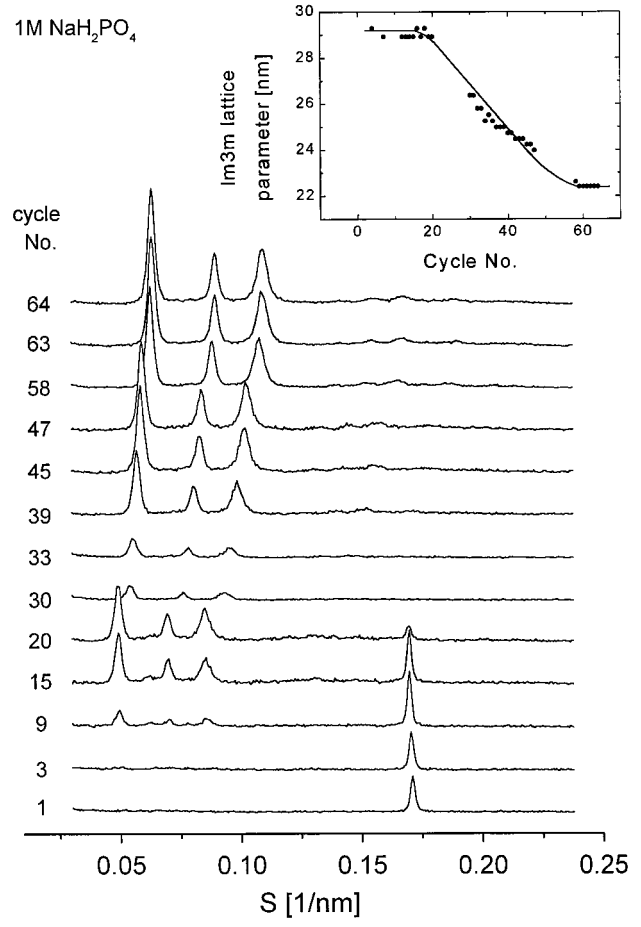

FIGURE 2 Conversion of 10 wt% DEPE dispersion in 1 M NaH_2PO_4 solution (pH 4.5) from lamellar into Im3m cubic phase during temperature cycling at 10°C/min in the range 43–83°C, with a wait time of 2 min at 43°C. The diffraction patterns shown were recorded at 43°C immediately before the next heating step. The Im3m lattice parameter as a function of the cycle number is given in the inset.

plete disappearance of the L_α phase in the heating step. With DEPE dispersions in 1 M NaSCN solutions, cubic phases were induced by temperature cycling between 75°C and 95°C. A trivial but worthwhile observation is that cycling within the limits of the L_α range does not result in cubic phase formation.

DEPE in water and ethylene glycol solutions

As shown by ^{31}P NMR, temperature cycling of DEPE/water dispersions through the L_α-H_{II} transition leads to the appearance and gradual increase of an isotropic signal, which was assumed to indicate cubic phase formation (Veiro et al., 1990). The present x-ray data corroborate this assumption. Temperature cycling of a 10 wt% DEPE dispersion at 10°C/min produced a cubic trace with three peaks positioned as $\sqrt{2}$:$\sqrt{4}$:$\sqrt{6}$ (Fig. 4 *A* and Table 1). These peaks become visible after ~10 cycles, and after 20 cycles their height is 1–2% of that of the L_α reflection. Even smaller cubic trace appeared after temperature cycling of a 37 wt%

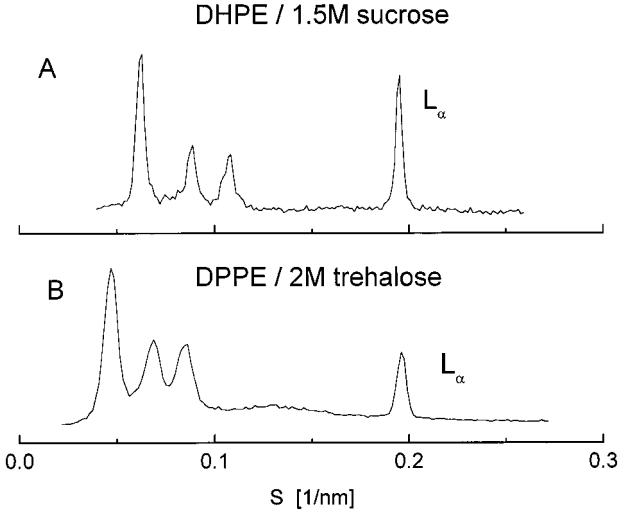

FIGURE 3 Coexistence of Im3m and L_α phases in 10 wt% DHPE and DPPE dispersions induced by temperature cycling. (*A*) DHPE/1.5 M sucrose after 18 cycles 76–94-76°C at 9°C/min with a 2-min wait time at 76°C (Im3m lattice parameter 23 nm at 76°C). (*B*) DPPE/2M trehalose after three cycles in the range 80–95°C at a scan rate of 1°C/min (Im3m lattice parameter 29 nm at 80°C).

DEPE dispersion in 1 M ethylene glycol solution (data not illustrated). More extended cycling of a 60 wt% DEPE dispersion executed by laser-flash T-jumps resulted in a pattern with several peaks on the low- and high-angle sides of the still strongly dominating L_α reflection (Fig. 4, *patterns B and inset*). This pattern is not consistent with a single cubic phase. By analogy with the Im3m/Pn3m cubic phase mixtures observed in certain conditions in the pres-

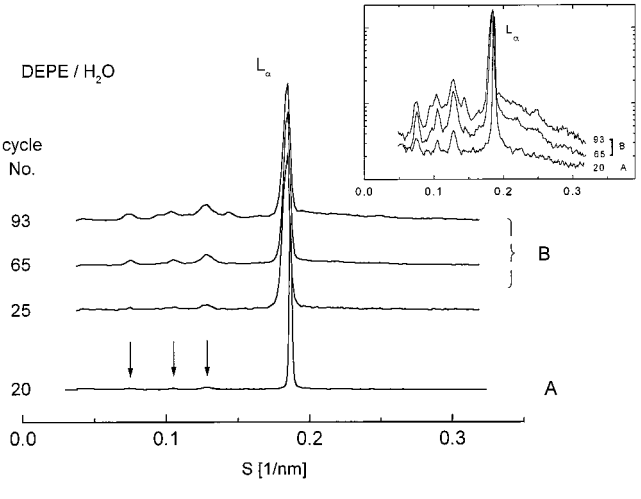

FIGURE 4 Diffraction patterns recorded from DEPE dispersions in distilled water subjected to temperature cycling. (*A*) 10 wt% DEPE after 20 cycles at 10°C/min in the range 51–71°C. The arrows show the positions of the emerging cubic phase reflections. (*B*) 60 wt% DEPE; temperature cycling executed by laser T-jumps from 55°C at 50-s intervals (SAXS and WAXS setup, wide-angle region not shown). The cycle numbers are indicated in the figure. An inset in logarithmic scale shows more clearly the induced cubic phase pattern. Tentative phase assignments are given in Table 1.

TABLE 1 Lattice parameters of cubic phases induced in DEPE dispersions by means of temperature cycling*

Solute	DEPE conc. [wt%]	Im3m (nm)		Pn3m (nm)	Ia3d (nm)
		Initial	Final		
Na_2SO_4, 1 M	10	34.5[#]	22.5 (68)	17.6[§]	—
Na_2SO_4, 0.2 M	10	24.0			—
NaH_2PO_4, 1 M	10	29.3	22.4 (68)	17.5[§]	—
NaCl, 1 M	10	26.0			—
NaSCN, 1 M	10	21.0	21.0 (27)	16.4[¶]	—
NaSCN, 0.2 M	10	20.9			—
Sucrose, 1 M	10	26.5	22.4 (22 T-jumps)	20.7[§]	—
Sucrose, 0.5 M	10	23.2			—
No (H_2O only)	10	19.0			—
Na_2SO_4, 1 M	30	34.6 (2)	—	27.0 (2)[¶]	26.6 (80)
NaH_2PO_4, 1 M	30	28.0 (10)	—	22.0 (10)[¶]	25.8 (51)
NaCl, 1 M	30	26.0 (10)	—	20.8 (10)[¶]	28.5 (35)
NaSCN, 1 M	30	20.2	20.2 (41)	16.0 (41)[¶]	—
No (H_2O only)	60	19.2 (93 T-jumps)		15.1 (93 T-jumps)[¶‖]	

*The data were obtained by uniform linear cycling at 10°C/min, unless otherwise indicated. The numbers in parentheses after the lattice parameters indicate the number of temperature cycles executed. The lattice parameter variations over the sample volumes were typically within ±0.3 nm. Empty fields correspond to missing data.

[#]In one preparation, an initial Im3m lattice parameter of 39.5 nm was recorded.

[§]Pn3m phase obtained by means of high-temperature Im3m → Pn3m transition.

[¶]Pn3m phase appearing in parallel with Im3m during the conversion process.

[‖]Tentative assignment.

ence of solutes (Fig. 6), it seems reasonable to consider it to be due to a mixture of similar type, with spacings given in Table 1. It is clear from these data that DEPE dispersions in excess water rather slowly convert to cubic phase when subjected to temperature cycling. In this respect, the behavior of DEPE is qualitatively similar to that of DOPE (Shyamsunder et al., 1988; Erbes et al., 1994). By contrast with DEPE and DOPE, m-DOPE dispersions in excess water are known to form, albeit slowly, cubic phases either spontaneously or in the presence of small amounts of impurities (Gruner et al., 1988; Siegel and Banschbach, 1990). In accord with these results, our x-ray measurements showed that m-DOPE in water, sodium salt, and sucrose solutions converts to cubic phase within a few, or even a single temperature cycle.

Formation of the Im3m cubic phase in 10 wt% DEPE dispersions in salt and sucrose solutions

With 10 wt% DEPE dispersions in 1 M sodium salt or sucrose, a series of 20–50 cycles at 10°C/min was sufficient for complete conversion from the lamellar to cubic phase (Figs. 2 and 5). In general, the characteristics of cubic phase formation in salt and sucrose solutions were similar. This process requires ~20 cycles in the presence of NaH_2PO_4, Na_2SO_4, and NaSCN, and about two times more cycles in NaCl and sucrose solutions at the same molar concentration. A decrease in the salt concentration to 0.2 M increases several times the number of cycles required for the conversion. A decrease in the sucrose concentration to 0.5 M also results in decreased conversion rate.

All solutes used induce formation of an Im3m cubic phase in 10 wt% DEPE dispersions. Well-resolved x-ray patterns of this phase were obtained for DEPE dispersions in NaH_2PO_4, Na_2SO_4, and sucrose solutions. They comprise 12–13 reflections in ratios of $\sqrt{2}$:$\sqrt{4}$:$\sqrt{6}$:$\sqrt{8}$:$\sqrt{10}$:$\sqrt{12}$:$\sqrt{14}$:$\sqrt{16}$:$\sqrt{18}$:$\sqrt{20}$:$\sqrt{22}$:$\sqrt{24}$:$\sqrt{26}$ (Fig. 6 *A1*), consistent with cubic aspect #8, extinction symbol I- - -; space group of highest symmetry Im3m (Q^{229}) (Kasper and Lonsdale, 1985). The reflection $\sqrt{8}$ was typically absent from or very

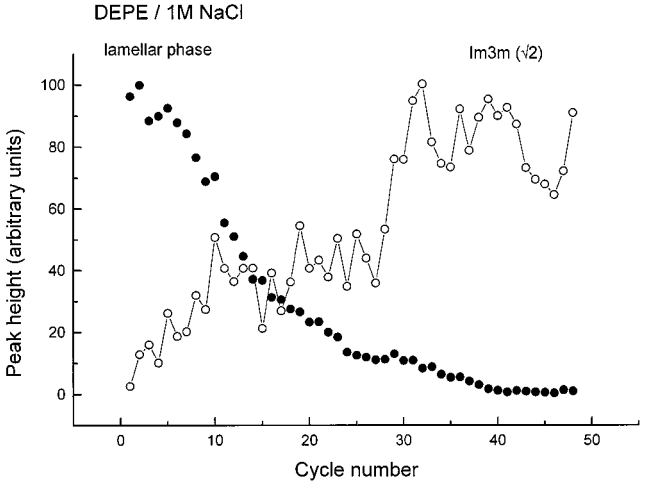

FIGURE 5 Decrease of the first-order L_α reflection and increase of the Im3m $\sqrt{2}$ reflection as a function of the temperature cycle number for 10 wt% DEPE dispersion in 1 M NaCl solution. Temperature cycling 46–64-46°C at a scan rate of 10°C/min. The Im3m lattice parameter is 26.0 nm (Table 1).

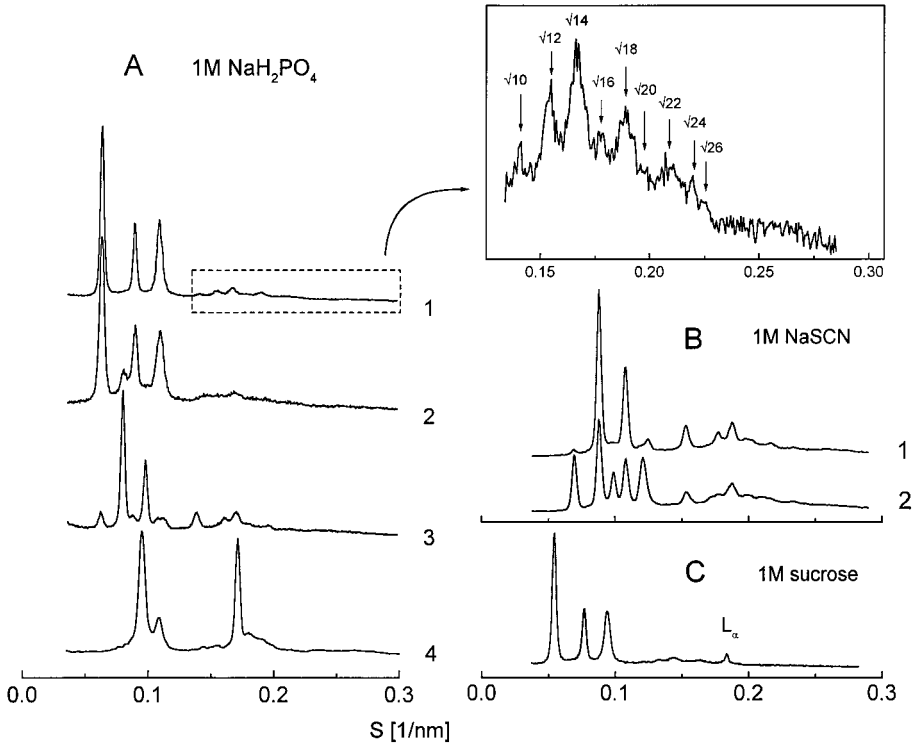

FIGURE 6 Selection of x-ray diffraction profiles of cubic phases induced in DEPE dispersions. (*A*) 1 M NaH_2PO_4 solution: 1. Im3m phase induced by temperature cycling at 10°C/min (10 wt% DEPE). 2. Im3m phase with an admixture of (possibly) Pn3m phase induced by laser-flash temperature cycling (10 wt% DEPE). 3. Pn3m phase obtained by heating of an Im3m phase through the Im3m → Pn3m transition shown in Fig. 7. A small residual amount of the Im3m phase is also visible (10 wt% DEPE). 4. Ia3d phase coexisting with the L_α phase (30 wt% DEPE). (*B*) 30 wt% DEPE/1M NaSCN: examples of coexisting Pn3m and Im3m phases with different intensity ratios recorded from different sample portions. (*C*) 10 wt% DEPE/1M sucrose: Im3m phase with a small residual amount of the L_α phase obtained by temperature cycling at 10°C/min.

weak in these patterns. As we found no references in published work, it is pertinent to note here a specific problem inherent to all Im3m assignments in lipid systems. The above reflection set coincides with that of cubic aspect #6, represented by a single space group, Pn3n (Q^{222}), except for the $\sqrt{21}$ reflection, which is forbidden in the former and permitted in the latter cubic aspect (a phase of Pn3n symmetry has not been reported so far for lipids). Thus it is not possible to distinguish between cubic aspects #6 and #8 from diffraction patterns containing less than at least the first 11 reflections. As a matter of fact, many of the published assignments of Im3m phases have been made on the basis of fewer than 10 low-angle reflections (for some of the few exceptions, see Caffrey, 1987; Mariani et al., 1988; Seddon et al., 1990). The low resolution of the respective x-ray patterns has usually been attributed to the liquid crystalline nature of the lipid phase. Even if based on more than 10 reflections, an Im3m identification is inevitably of the "negative" kind, as it hangs solely on the absence of the $\sqrt{21}$ reflection. Such an absence does not necessarily mean, however, that the reflection is forbidden. Because, in addition, the reflections above $\sqrt{18}$ are typically very weak (Fig. 6, *inset*; see also table 1 in Mariani et al. 1988), a reliable distinction between forbidden and weak, unobservable reflections in this range appears even more problematic. In view of this difficulty, it is desirable to have independent confirmation for an Im3m assignment. Mariani et al. (1988) refer to freeze-fracture and image reconstruction data verifying their choice of Im3m space group for a monoolein/cytochrome C/water system. We believe that additional support for our Im3m assignments follows from the lattice parameter ratio of the Im3m and Pn3m cubic phases being in agreement with their description with infinite periodic minimal surfaces (see Discussion).

After conversion to the cubic phase, the samples were scanned by moving them with respect to the incident x-ray beam. Except as a check for radiation damage effects, another reason to systematically perform such scans was that, in comparison to phosphatidylcholines, the PEs are known to hydrate less and to form less homogeneous dispersions in an excess of water. However, we were unable to detect other phases coexisting with the Im3m phase. Over the sample volumes, the Im3m lattice parameter was found to vary in an unsystematic way within a range of several angstroms. These variations were small with respect to the lattice parameter (within 2–3%) and were not analyzed in detail.

Initial cubic phase and relaxation of the lattice parameter

The initial cubic phase appearing in 10 wt% DEPE/solute dispersions during the first several temperature cycles has a higher lattice parameter that gradually relaxes to a smaller value (Figs. 1 and 2). Upon cycling at 10°C/min, the initial lattice parameter remains constant until complete disappearance of the L_α phase and only then starts to decrease (Fig. 2, *inset*). We designate as "initial" the cubic lattice parameters determined while the L_α phase is still visible, as in Fig. 6 *C*, or immediately after its disappearance. The initial lattice parameters are summarized in Table 1. The initial

Im3m lattice parameters for DEPE dispersions in 1 M Na_2SO_4 and NaH_2PO_4 solutions are remarkably large and possibly represent the largest values reported for lipid cubic phases. These large initial spacings strongly decrease, however, with a decrease in solute concentration (Table 1).

To obtain the "final" Im3m spacings requires more extensive temperature cycling, and we have determined them in a limited number of cases, whenever the relaxation process reached a plateau (Fig. 2, *inset*; Table 1). It is noteworthy that no such relaxation takes place in the DEPE/NaSCN system. In that case the initial and final cubic lattice parameters coincide. It is also worth noting that the latter spacings were the smallest among all solutes studied and were close to the values found for DEPE/water dispersions.

In many cycling experiments at a scan rate of 10°C/min, the pattern emerging during the first several cycles was not that of an Im3m phase, but rather of its mixture with another phase, most likely a Pn3m phase. With an increase in the cycle number, the reflections originating from the second phase gradually disappeared and gave way to a single Im3m x-ray pattern. Poorly resolved contributions from a possible Pn3m phase were also present in the cubic patterns produced by means of laser-flash temperature cycling (Fig. 6 *A2*).

Temperature dependence of the cubic phases in 10 wt% DEPE dispersions: Im3m → Pn3m transition

An important question arising in this study concerns the possible occurrence of structures mediating cubic phase formation. To address this question, we recorded sequences of x-ray patterns at short time intervals within the individual cycles but were unable to detect structures different from L_α, H_{II}, and an increasing cubic phase pattern. However, the background scattering at the low-angle (beam stop) end of the x-ray patterns was found to monotonously decrease with the system evolution from the lamellar into the cubic phase (Fig. 1). The emerging cubic phases displayed a peculiar temperature dependence—their lattice parameters were constant in the temperature range of the L_α phase, but exhibited strong and rapidly reversible shrinking with the temperature in the H_{II} range. Temperature scans performed with DEPE dispersions fully converted into the cubic phase revealed identical temperature dependence—a reversible decrease with temperature in the H_{II} range and constancy with temperature in the L_α range. Except for DEPE in NaH_2PO_4 (Figs. 7 and 8 *A*), we observed such a temperature dependence also for the cubic phases in DEPE/sucrose, DEPE/Na_2SO_4, and DHPE/sucrose preparations (data not shown). Erbes et al. (1994) report similar dependencies for the Im3m and Pn3m phases induced in DOPE dispersions. One may expect that the strong shrinkage of the cubic lattices at higher temperatures, as opposed to their constancy in the L_α range, manifests an increased propensity for interfacial curvature in the H_{II} range. However, clarification of this effect requires extensive quantitative analysis.

Upon heating to high temperatures, the reflections originating from the Im3m phase disappear at ~85°C. They are replaced by a different set of reflections that gradually move to higher spacings during the subsequent cooling scan. These reflections abruptly become temperature-insensitive in the L_α temperature range (Figs. 7 and 8 *A*). The new pattern comprises 12 reflections in ratios $\sqrt{2}:\sqrt{3}:\sqrt{4}:\sqrt{6}:\sqrt{8}:\sqrt{9}:\sqrt{10}:\sqrt{11}:\sqrt{12}:\sqrt{14}:\sqrt{16}:\sqrt{17}$, consistent with cubic aspect #4 (space groups Pn3m/Pn3) (Kasper and Lonsdale, 1985). A small amount of Im3m phase reappears in the diffraction patterns and coexists with the Pn3m phase when

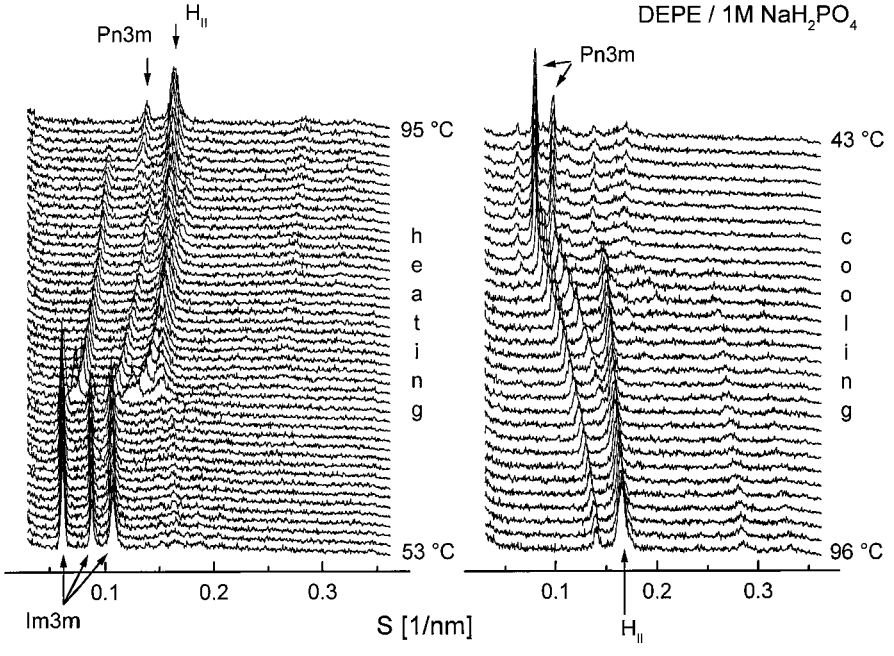

FIGURE 7 Temperature dependence of the Im3m (heating scan) and Pn3m (cooling scan) phases in 10 wt% DEPE dispersion in 1 M NaH_2PO_4 solution. An Im3m → Pn3m transition takes place at ~85°C (*left*). The lattice parameters of the cubic phases are given in Fig. 8.

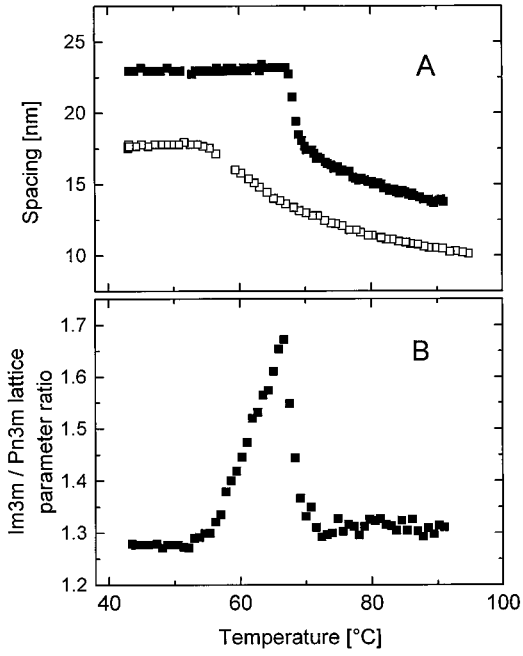

FIGURE 8 Temperature dependence of the Im3m (heating scan) and Pn3m (cooling scan) lattice parameters for a 10 wt% DEPE dispersion in 1 M NaH_2PO_4 solution (*A*). (*B*) Im3m/Pn3m lattice parameter ratio.

the cooling scan enters the L_α range (Fig. 7, *right*; Fig. 6 *A3*). Its lattice parameter is identical to that of the initial Im3m phase. The mixture of the two phases appears to be stable in the sense that several successive cycles at 10°C/min up to ~100°C did not further reduce the Im3m trace and did not influence their spacings. These data indicate that a cooperative transition of Im3m to Pn3m takes place at ~85°C. The Im3m and Pn3m lattice parameters determined, respectively, from the heating and cooling scans in Fig. 7, are given in Fig. 8. Their ratio in the L_α range is equal to 1.28 ± 0.01. Similar to samples with single Im3m phase, the Im3m and Pn3m lattice parameters also exhibited random variations within several angstroms between different sample portions. It is interesting to note that these variations were tightly coupled in such a way that the lattice parameter ratio of the coexisting Im3m and Pn3m phases always remained equal to 1.28. The temperature dependence of this ratio is given in Fig. 8 *B*. In the H_{II} region, it was calculated by dividing the Im3m lattice parameter, determined from the heating scan, into the Pn3m lattice parameter, determined from the subsequent cooling scan. Similar Im3m → Pn3m transitions take place in 10 wt% DEPE dispersions in 1 M Na_2SO_4 and 1 M sucrose solutions (we did not perform such experiments with DEPE dispersions in NaCl solutions). A more detailed description of the Im3m → Pn3m transition, furnished with microcalorimetric characterization, will be published subsequently.

In DEPE dispersions fully converted into cubic phase, i.e., after complete abolishment of the L_α phase, an H_{II} phase is still present and coexists with the cubic phase (Fig. 7). This phase cannot be eliminated by further temperature cycling. Because the residual H_{II} phase does not revert to the L_α phase, but just disappears from the x-ray pattern upon cooling, it should then convert either to the cubic phase or to some indiscernible disordered state. An H_{II} phase was reported to convert to cubic phase in DOPE dispersions as well (Shyamsunder et al., 1988; Erbes et al., 1994). The present data provided no clue to the reason why the residual H_{II} phase does not revert to the L_α phase, in contrast to the behavior of the initial H_{II} phase.

DEPE dispersions in NaSCN solutions

In the presence of 1 M NaSCN, the nascent phase replacing the L_α phase upon temperature cycling is not a single cubic phase. Its x-ray pattern has a structure identical to that recorded for the Im3m/Pn3m mixtures obtained after heating through the Im3m → Pn3m transition. It divides into two subsets of reflections typifying an Im3m and a Pn3m phase (Fig. 6 *B*). These two phases steadily coexist in the whole L_α range from 85°C to 35°C. The Im3m/Pn3m intensity ratio, recorded in different samples and from different portions of the same sample, strongly varied, as illustrated by the two patterns in Fig. 6 *B*. We utilized these intensity variations to distinguish more clearly between the reflection sets of the Im3m and Pn3m phases. Their lattice parameter ratio was within the range 1.26–1.28. Similar to the results obtained for Im3m/Pn3m mixtures in other solutions, the lattice parameter variations were surprizingly synchronous for the two coexisting cubic phases.

The temperature cycling of DEPE/1 M NaSCN dispersions was typically executed in the range 75–95°C for the reason that the L_α-H_{II} transition in these dispersions takes place at 85°C. Because T_{max} exceeds the temperature of the Im3m → Pn3m transitions observed with other solutes (Fig. 7), we do not associate the formation of Im3m/Pn3m mixtures in 1 M NaSCN solutions with some specific property of this salt, but rather consider it a possible consequence of an Im3m → Pn3m transition taking place in this system as well. Support for this conclusion was obtained from measurements on 10 wt% DEPE dispersions in a more diluted (0.2 M) NaSCN solution. In that case, the L_α-H_{II} transition takes place at ~70°C. Accordingly, the temperature cycling was executed in the range 55–75°C, with T_{max} below the Im3m → Pn3m transition temperature. Such cycling resulted in the appearance of an Im3m phase accompanied by no trace of the Pn3m phase (Table 1).

Effect of higher DEPE concentrations on cubic phase formation

Both the degree of conversion and the structure of the newly formed cubic phase strongly depend on the DEPE concentration. At higher DEPE contents (30 ± 5 wt% of lipid), cubic phase formation is hindered after 20–30 temperature cycles (Fig. 9). The conversion does not go through, but reaches a stage with coexisting cubic and L_α phases. The

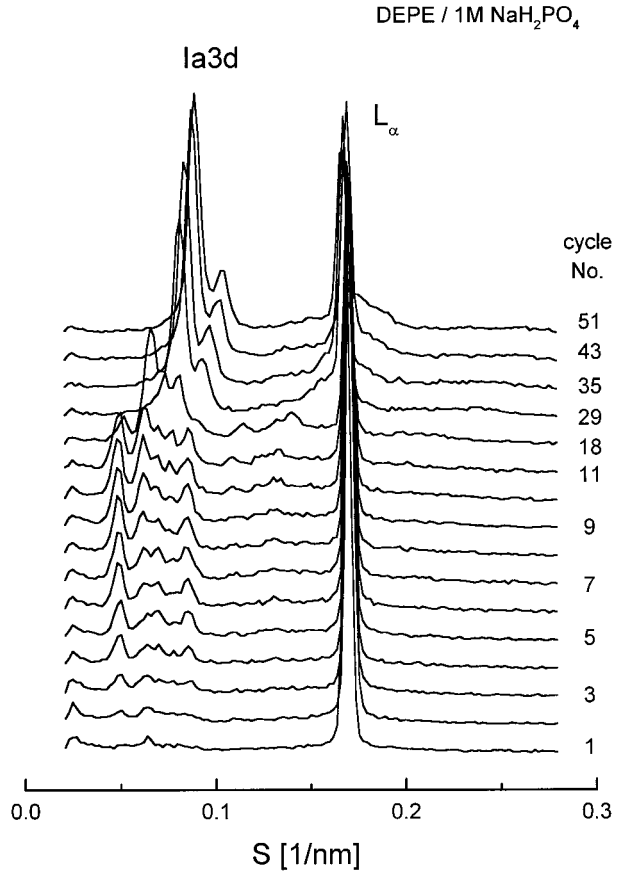

FIGURE 9 Hindered conversion of a 30 wt% DEPE dispersion in 1 M NaH_2PO_4 solution from the L_α phase into the Ia3d cubic phase upon temperature cycling in the range 45–75°C at 10°C/min. The sequence of the diffraction frames shown was recorded at 45°C immediately before the next heating step.

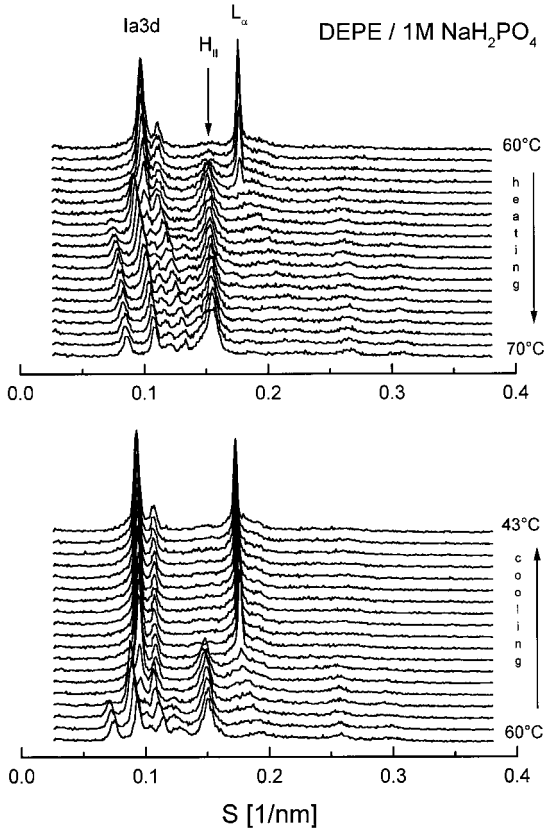

FIGURE 10 Reversible transformation of an Ia3d cubic phase, coexisting with an L_α phase, into a mixture of (presumably) Im3m and Pn3m phases, coexisting with an H_{II} phase; 30 wt% DEPE dispersion in 1 M NaH_2PO_4 solution. Scan rate 1°C/min.

cubic phase at this stage indexes as a Ia3d phase with prominent $\sqrt{6}$ and $\sqrt{8}$ peaks and smaller $\sqrt{14}$, $\sqrt{16}$, $\sqrt{22}$, $\sqrt{24}$, $\sqrt{26}$ reflections (Fig. 6 *A4*). The $\sqrt{20}$ reflection is not observable, as it happens to overlap with the large first-order reflection of the L_α phase. We observed such partial conversions of the L_α phase into Ia3d phase for DEPE dispersions in 1 M NaH_2PO_4, Na_2SO_4, and NaCl solutions, but not for dispersions in 1 M NaSCN solution (Table 1). It is pertinent to note that initially, during the first several temperature cycles, an Im3m/Pn3m mixture appears to emerge in these dispersions (Fig. 9 and Table 1). With continuation of the cycling, the initial phase gradually transforms into Ia3d phase while, at the same time, the conversion rate decreases virtually to zero.

Heating of the Ia3d phase results in precipitous transformation of its x-ray pattern into a different pattern at about the temperature of the L_α-H_{II} phase transition (Fig. 10, *top*). This transformation is readily reversible, and both the Ia3d phase and the L_α phase fully recover upon cooling (Fig. 10, *bottom*). The high-temperature x-ray pattern contains five more visible reflections that do not appear to index as a single cubic phase. A line of reasoning based on the relation between coexisting Im3m and Pn3m phases (see Discussion) suggests, however, that it might result from a mixture of these two phases. In accord with such a premise, the five discernible reflections consistently divide into a set with the first three Im3m reflections ($\sqrt{2}$:$\sqrt{4}$:$\sqrt{6}$) and a set with the first two Pn3m reflections ($\sqrt{2}$:$\sqrt{3}$), with a Im3m/Pn3m lattice parameter ratio close to 1.28 (Fig. 11). In further support of this interpretation, upon heating to higher temperatures, the Im3m reflections disappear at ~85°C and do not reappear in subsequent cooling, apparently because of a high-temperature Im3m → Pn3m transition of the kind shown in Fig. 7. The Ia3d lattice parameter is insensitive to temperature in the L_α range, whereas the cubic phases in the H_{II} range exhibit negative temperature dependence (Figs. 10 and 11).

Stability of the induced cubic phases and conversion into the lamellar gel state

With storage of the induced cubic phases for up to 10 h at temperatures in the L_α range (40–50°C), their diffraction patterns did not change, and no L_α phase reappeared. Incubations for 5–10 min at 100°C also did not eliminate the cubic phase. Upon cooling to room temperature, the cubic

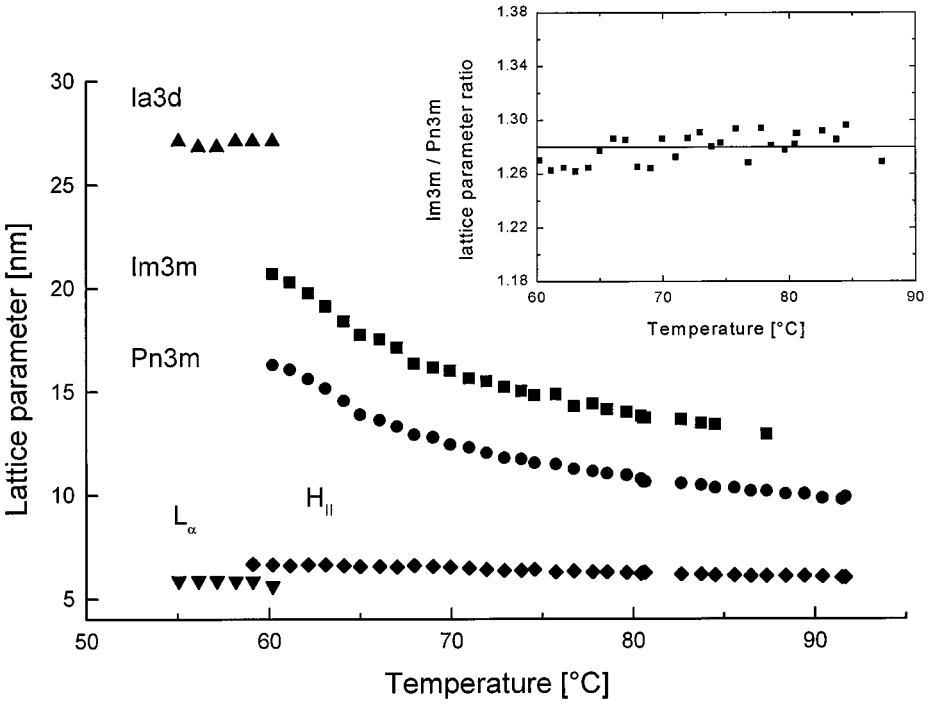

FIGURE 11 Lattice parameters of the cubic phases in 30 wt% DEPE dispersion in 1 M Na_2SO_4 solution as a function of temperature. Heating scan rate 2°C/min. The inset shows the Im3m/Pn3m lattice parameter ratio.

phases convert to the lamellar gel phase at the temperature of the liquid crystalline-to-gel transition. A typical example for the evolution of the diffraction patterns during the latter transition is given in Fig. 12. If heated, the gel phase converts to the L_α phase. Recovery of the L_α phase after cooling to gel state is also known to take place in DOPE converted to the cubic phase (Shyamsunder et al., 1988). During the conversion from the lamellar to cubic phase, the DEPE dispersions gradually become transparent. Upon cooling to the gel phase, they become turbid again, but their texture appears to be different from that of the initial gel phase. This effect was especially clear for 10 wt% DEPE samples in capillaries where the lipid was curled in a characteristic spiral pattern with a step of 2–3 mm along the capillary long axis. This pattern usually disappears after storage of the capillaries at room temperature.

DISCUSSION

The PEs are an abundant phospholipid class in the native membranes, and it is clearly of interest that physiologically relevant solutes, such as NaCl, sucrose, and trehalose, facilitate their transformation into cubic phase. Aqueous dispersions of the presently studied lipids, DEPE, DHPE, and DPPE, do not spontaneously form cubic phases in isothermal conditions. Whereas it might be possible to convert these dispersions to cubic phase by means of extensive temperature cycling, this process strongly accelerates in the presence of sodium salts and disaccharides. The experiments carried out with these PEs agree on the general features of the acceleration effect. Recently we also observed accelerated formation of cubic phases for DOPE and dipalmitoleoyl PE (work in progress). We assume on these grounds that a solute-accelerated transformation into cubic phase is a general property of the PEs and that it might be found in other lipid systems as well. The present results may have relevance to specific biological issues involving high solute concentrations, for example, issues related to cryo-

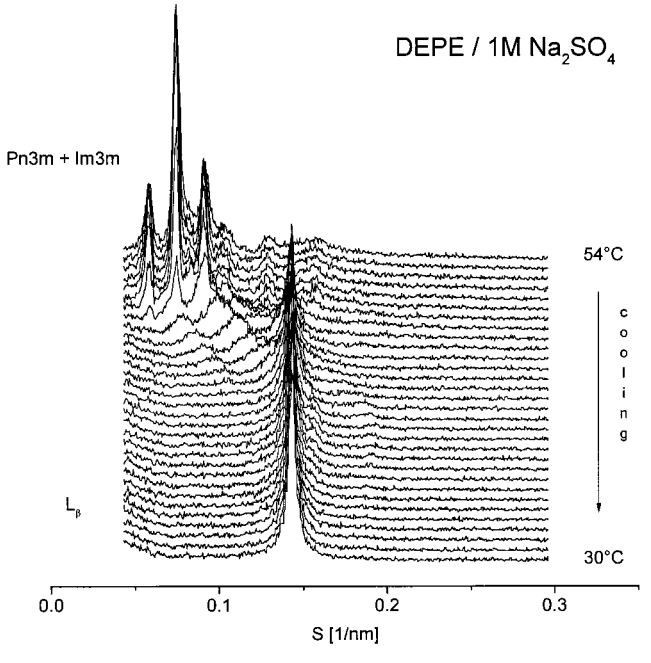

FIGURE 12 Conversion of an Im3m/Pn3m cubic phase mixture into the lamellar gel phase upon cooling at 1°C/min. 10 wt% DEPE dispersion in 1 M Na_2SO_4 solution.

biology. Cellular and extracelullar solutes are known to concentrate to molar concentrations at extreme conditions, such as dehydration and low temperatures leading to freezing of tissue water. Furthermore, the dissacharides trehalose and sucrose are native cryoprotectants. The ability of some organisms to survive complete dehydration (anhydrobiosis) correlates with enhanced synthesis of these sugars up to very high concentrations before dehydration and their degradation during subsequent rehydration (Clegg, 1965; Clegg et al., 1982; Madin and Crowe, 1975). With lipid compositions regulated in such a way as to keep the cellular membranes in the vicinity of a lamellar-cubic transformation (Lindblom and Rilfors, 1990), such environments of highly concentrated solutions might quickly bring about radical membrane reorganizations similar to those described here for model systems.

The 10 wt% DEPE dispersions studied here represent a suitable system for investigations on a relatively well-resolved, single Im3m cubic phase. As known from experience with other lipid systems (Caffrey, 1987), this phase is sometimes difficult to obtain in a reproducible manner, and its stability in excess water could be questioned. Except for studies on lipid/water systems, the present method for accelerated formation of cubic phases with relatively well-resolved x-ray patterns may find various other applications.

Role of solute type

The sodium salts used in the present work cover the whole range of the lyotropic series, with Na_2SO_4 and NaH_2PO_4 at the kosmotropic end, and NaSCN at the chaotropic end. One might expect that NaSCN would be a more efficient promoter of cubic phase formation, as it strongly expands the L_α range of DEPE at the expense of the H_{II} phase and provides, in this way, more space for formation of intermediary cubic structures. However, the salts Na_2SO_4 and NaH_2PO_4, which tend to depress the L_α range in favor of the H_{II} phase, turned out to be similarly efficient promoters. Kosmotropic solutes such as sucrose and trehalose also strongly facilitate the conversion to cubic phase. It is worth noting that ethylene glycol does not have an accelerating effect at all. Thus the acceleration effect does not appear to correlate, at least in an obvious way, with the solute arrangement in lyotropic series. A parameter that might correlate with such an arrangement seems to be the lattice parameter of the initial cubic phases. It is larger for the kosmotropic salts Na_2SO_4 and NaH_2PO_4 in comparison to the chaotropic salt NaSCN (Table 1).

Im3m/Pn3m lattice parameter ratio

A description frequently used in recent studies of bicontinuous cubic phases is their representation as lipid bilayers draped along infinite periodic minimal surfaces (IPMS) with cubic symmetry (for reviews see, e.g., Andersson et al., 1988; Lindblom and Rilfors, 1989; Seddon and Templer, 1995; Charvolin and Sadoc, 1996). In an IPMS representation, the Pn3m, Im3m, and Ia3d phases correspond to the diamond (D), primitive (P), and gyroid (G) surfaces, respectively. Based on considerations following from the Bonnet transformation between these surfaces (Hyde et al., 1984), the unit cell dimensions of these phases in the states of cubic-cubic coexistence could be expected to satisfy the ratio D:P:G = 1:1.28:1.58. It is interesting to point out that the Im3m and Pn3m phases induced in DEPE dispersions appear to comply with such an IPMS representation.

The present data allow us to determine with good accuracy the lattice parameter ratios of steadily coexisting Im3m and Pn3m cubic phases in the L_α range, where their lattice parameters are temperature-insensitive. The lattice parameter ratios determined from several patterns with the best resolution were invariably within the range 1.280 ± 0.005. In most other cases the deviation from 1.28 did not exceed ± 0.01. We consider this agreement with the theoretical value as providing support for the identification of the cubic phases induced in 10 wt% DEPE dispersions as Im3m and Pn3m cubic phases, as well as for their representation with IPMS.

While staying constant in the L_α range, the dimensions of these two phases strongly shrink with the temperature in the H_{II} range (Fig. 8 *A*). Nevertheless, the Im3m/Pn3m lattice parameter ratio in the latter range remains very close to the theoretical value (Fig. 8 *B*). The strong deviation from 1.28 at temperatures around 65°C obviously associates with the heating-cooling hysteresis seen in Fig. 8 *A*. At temperatures above 70°C, the ratio assumes values about 1.30, only slightly above 1.28. Because we divide Im3m spacings obtained from a heating scan by Pn3m spacings obtained from a subsequent cooling scan, the possibility cannot be excluded that this discrepancy results from a kinetic lag of the lattice parameters at a scan rate of 1°C/min. Above the Ia3d transition into a mixture of presumably Im3m and Pn3m phases (Fig. 10), the Im3m/Pn3m lattice parameter ratio is in the range 1.28 ± 0.02, again in good accord with the theoretical value (Fig. 11, *inset*).

It thus appears that the Im3m and Pn3m phases preserve their structures up to high temperatures. That their lattice parameter ratio is close to 1.28 during the Im3m $\rightarrow$ Pn3m transition does not necessarily imply, however, that this transition should be considered as materialization of the Bonnet transformation between the respective P and D surfaces. The Bonnet transformation relates the P, G, and D surfaces in the sequence P $\leftrightarrow$ G $\leftrightarrow$ D via intermediate self-intersecting minimal surfaces, whereas we observe a cooperative, seemingly direct Im3m $\rightarrow$ Pn3m transition with no evidence for an intermediate Ia3d phase (the G surface). As pointed out (Seddon and Templer, 1995), a Bonnet-like transformation between cubic phases represented by IPMS appears unphysical, as it would involve lipid bilayer self-intersections. A possibility for direct Im3m $\rightarrow$ Pn3m transformation has been given by Sadoc and Charvolin (1989). It can be visualized as pulling apart the octahedral tunnel joint of an Im3m unit cell into two tetra-

hedral joints of Pn3m cells. Such reshaping of an Im3m node into two Pn3m nodes has the advantage of not requiring bilayer self-intersections (Seddon and Templer, 1995). It is consistent with the 1.28 Im3m/Pn3m lattice parameter ratio, as can readily be seen by comparing the specific areas of the Im3m and Pn3m unit cells (2.345 and 1.919, respectively; Mackay, 1985). With a lattice parameter ratio of 1.28, the lipid bilayer enclosed within one Im3m cell equals that enclosed within exactly two Pn3m cells.

Cubic phase progression in the excess water range

The lipid phases are usually considered as fully hydrated when the temperatures of their L_β-L_α-H_{II} transitions become independent of the water content. In this sense, the present measurements were carried out with PE dispersions in a large excess of water. As could be expected from the higher water content of the cubic phases, they revealed, however, a strong dependence of the process of lamellar-to-cubic conversion on the lipid concentration. This dependence is represented by the following transition schemes:

10 wt% DEPE dispersions in 1M sodium salt (except for NaSCN) and sucrose solutions:

$$L_\alpha \overset{\text{T-cycling}}{\sim\sim\sim} Im3m \overset{\sim 65^\circ C}{\longleftrightarrow} Im3m_t + H_{II} \overset{\sim 85^\circ C}{\longrightarrow} Pn3m_t + H_{II}$$

30 wt% DEPE dispersions in 1M NaH_2PO_4, Na_2SO_4, and NaCl solutions:

$$L_\alpha \overset{\text{T-cycling}}{\sim\sim\sim} Ia3d + L_\alpha \overset{\sim 65^\circ C}{\longleftrightarrow} Im3m_t + Pn3m_t + H_{II}$$

10-30 wt% DEPE dispersions in 1M NaSCN (high-temperature cycling):

$$L_\alpha \overset{\text{T-cycling}}{\sim\sim\sim} Pn3m + Im3m$$

The subscript t refers to cubic phases with temperature-dependent lattice parameters.

As the DEPE content was increased from 10 wt% to ~30 wt% in 1 M NaH_2PO_4, Na_2SO_4, and NaCl solutions, the Im3m phase was replaced with an Ia3d phase, and the lamellar-to-cubic conversion was hindered at a stage with coexisting Ia3d and L_α phases. In principle, this effect is not surprising, as it is known that the Ia3d phase requires less water and forms at the lowest water contents in comparison to the Im3m and Pn3m phases. The position of the Pn3m phase in this progression remains unclear. In many experiments, it seemed to appear during the first several temperature cycles, in coexistence with the Im3m phase. However, with an increase in the cycle number, the Pn3m trace disappeared, giving way either to the Im3m phase in 10 wt% DEPE dispersions, or to the Ia3d phase in 30 wt% DEPE dispersions. Recently, theoretical models for the relative stability of the inverse bicontinuous cubic phases have been proposed, based on evaluations of the bilayer elastic energy (Templer et al., 1994, 1995; Chung and Caffrey, 1994). According to these models, the cubic phases arrange in the order Im3m → Pn3m → Ia3d with a decrease in water content, as a consequence of their space-filling properties. The Pn3m phase was predicted to be stable in a very narrow range of water contents (~2 wt%) between the stability ranges of the Im3m and Ia3d phases. It is clear, however, that temperature is another, not less important determinant of their stability. In the present experiments, a Pn3m phase was found to form via Im3m → Pn3m transition at high temperatures. Similarly, in the excess water range of didodecyl PE, a Pn3m phase was found to replace the Im3m phase at higher temperatures (Seddon et al., 1990). Because the Im3m → Pn3m transition in DEPE dispersions is not reversible (or only partially reversible), it is clear that conclusions regarding the Im3m and Pn3m stability at a given hydration level should be preceded by careful assessment of the specimen temperature prehistory, i.e., whether the lipid dispersion has been driven through a transition of the above kind.

Possible mechanism of the acceleration effect

Because the cubic phases induced in DEPE dispersions by temperature cycling do not display a tendency toward isothermal relaxation into the lamellar liquid crystalline state, it is unclear which of the two phases is the thermodynamically stable one. As has been argued for DOPE dispersions (Shyamsunder et al., 1988), it seems reasonable to assume for DEPE dispersions as well that the lack of observable isothermal interconversions between their L_α and cubic states is associated with a large kinetic barrier imposed by their different geometries. The cubic phases induced in DEPE dispersions are typified by large lattice parameters (Table 1). For such highly swollen bicontinuous cubic phases, where the lipid bilayers are at relatively large separations, the leading term defining their local stability minimum might be expected to be the curvature elastic energy (Templer et al., 1994). On the other hand, on the basis of the general ideology of the Derjaguin-Landau-Verwey-Overbeek (DLVO) theory, the free energy minimum for the L_α phase, where the lipid bilayers are closely stacked, would appear to be largely controlled by the balance of attractive and repulsive interlamellar interactions.

Within the framework of this scheme, one may speculate that the accelerating solutes serve to reduce the stability of the L_α phase and thus facilitate its conversion to cubic phase. Such an approach to the origin of their effect appears to emerge from the evidence for changes in the level of the background low-angle scattering that accompanies the PE phase transitions in sugar and salt solutions. These levels are higher for the PE gel and liquid-crystalline lamellar phases and strongly decrease during the L_α-H_{II} transition (Tenchov et al., 1996). A decrease in the level of the background scattering at low angles also accompanies the lamellar-to-

cubic conversion (Fig. 1). These data appear to indicate that the accelerating solutes destabilize to some extent the L_α phase and maintain certain lipid portions in a state of separated by larger spaces and uncorrelated bilayers. Such a conclusion is in agreement with the results of a freeze-fracture examination of DEPE/sucrose/water systems (H. W. Meyer, unpublished observations). Thus the state of the studied lipid dispersions before their conversion to the cubic phase may be represented as a mixture of organized multilamellar phase and uncorrelated, single bilayers. We consider these disordered bilayers a more likely source for formation of cubic phases on the ground that the attractive interactions in a well-stacked lamellar phase, which could be expected to impede the formation of a bicontinuous cubic phase, would be much weaker between bilayers separated by larger spaces. Because, according to models of the lamellar to inverted hexagonal phase transition (Caffrey, 1985; Siegel, 1986a–c), the single lipid bilayers should be less inclined to form an H_{II} phase, it may be further speculated that the heating-cooling cycles, driving the system through the L_α-H_{II} transition, serve in this case as a factor curving the single bilayers into shapes more adapted for the formation of an inverse bicontinuous cubic phase.

Studies on some other systems also show that disordered phases accompany cubic phase formation. A slow disordering of the m-DOPE lamellar phase was shown to precede the formation of the cubic phase in this lipid (Gruner et al., 1988; Siegel and Banschbach, 1990). The PC/fatty acid mixtures at specific molar ratios provide additional examples that the location of the cubic phases in their temperature-composition phase diagrams is closely associated with regions of broad, unresolved low-angle scattering from uncorrelated structures (Koynova et al., 1988, 1997b). While an involvement of uncorrelated, single lipid bilayers in mediating the process of solute-accelerated cubic phase formation appears possible on the basis of the present data, a further verification of this hypothesis would require a systematic, precise determination of the low-angle background scattering by methods similar to those developed for studies of x-ray scattering from protein solutions.

BT and RK acknowledge support from the EMBL Outstation at DESY, Hamburg, and from grant K-407/94 of the Bulgarian National Science Foundation.

REFERENCES

Andersson, S., S. Hyde, K. Larsson, and K. Lidin. 1988. Minimal surfaces and structures: from inorganic and metal crystals to cell membranes and biopolymers. *Chem. Rev.* 88:221–242.

Bogdanov, M., J. Z. Sun, H. R. Kaback, and W. Dowhan. 1996. A phospholipid acts as a chaperone in assembly of a membrane transport protein. *J. Biol. Chem.* 271:11615–11618.

Boulin, C., R. Kempf, M. H. J. Koch, and S. M. McLaughlin 1986. Data appraisal, evaluation and display for synchrotron radiation experiments: hardware and software. *Nucl. Instrum. Methods.* A249:399–407.

Caffrey, M. 1985. Kinetics and mechanism of the lamllar gel/lamellar liquid crystal and lamellar/inverted hexagonal phase transition in phosphatidylethanolamine: a real-time X-ray diffraction. *Biochemistry.* 24:4826–4844.

Caffrey, M. 1987. Kinetics and mechanism of transitions involving the lamellar, cubic, inverted hexagonal and fluid isotropic phases of hydrated monoacilglycerides monitored by time-resolved X-ray diffraction. *Biochemistry.* 26:6349–6363.

Charvolin, J., and J.-F. Sadoc. 1996. Ordered bicontinuous films of amphiphiles and biological membranes. *Philos. Trans. R. Soc. Lond. A.* 354:2173–2192.

Chung, H., and M. Caffrey. 1994. The curvature elastic energy function of the lipid-water cubic mesophase. *Nature.* 368:224–226.

Clegg, J. S. 1965. Origin of trehalose and its significance during formation of encysted dormant embryos of Artemia. *Comp. Biochem. Physiol.* 14:135–138.

Clegg, J. S., P. Seitz, W. Seitz, and C. F. Hazlewood. 1982. Cellular responses to extreme water loss: water replacement hypothesis. *Cryobiology.* 19:306–316.

de Kruijff, B. 1997. Lipids beyond the bilayer. *Nature.* 386:129–130.

Epand, R. M., and M. Bryszewska. 1988. Modulation of the bilayer to hexagonal phase transition and solvation of phosphatidylethanolamines in aqueous salt solutions. *Biochemistry.* 27:8776–8779.

Erbes, J., C. Czeslik, W. Hahn, R. Winter, M. Rappolt, and G. Rapp. 1994. On the existence of bicontinuous cubic phases in dioleoylphosphatidylethanolamine. *Ber. Bunsenges. Phys. Chem.* 98:1287–1293.

Fontell, K. 1990. Cubic phases in surfactant and surfactant-like lipid systems. *Colloid Polym. Sci.* 268:264–285.

Gagne, J., L. Stamatatos, T. Diacovo, S. W. Hui, P. L. Yeagle, and J. R. Silvius. 1985. Physical properties and surface interactions of bilayer membranes containing N-methylated phosphatidylethanolamine. *Biochemistry.* 24:4400–4408.

Gabriel, A. 1977. Position-sensitive x-ray detector. *Rev. Sci. Instrum.* 48:1303–1305.

Gruner, S. M., M. W. Tate, G. L. Kirk, P. T. C. So, D. C. Turner, D. T. Keane, C. P. S. Tilcock, and P. R. Cullis. 1988. X-ray diffraction study of the polymorphic behavior of N-methylated dioleoylphosphatidylethanolamine. *Biochemistry.* 27:2853–2866.

Hyde, S., S. Andersson, B. Ericsson, and K. Larsson. 1984. A cubic structure consisting of a lipid bilayer forming an infinite periodic minimum surface of the gyroid type in the glyceromonooleate-water system. *Z. Krystallogr.* 168:213–219.

Kasper, J. S., and K. Lonsdale, editors. 1985. International Tables for X-ray Crystallography, Vol. 2. 1985. D. Riedel Publishing Company, Dordrecht, the Netherlands.

Koynova, R., J. Brankov, and B. Tenchov. 1997a. Modulation of the lipid phase behavior by low-molecular solutes. *Eur. Biophys. J.* 25:261–275.

Koynova, R., and M. Caffrey. 1994. Phases and phase transitions of the hydrated phosphatidylethanolamines. *Chem. Phys. Lipids.* 69:1–34.

Koynova, R. D., B. G. Tenchov, P. J. Quinn, and P. Laggner. 1988. Structure and phase behavior of hydrated mixtures of L-dipalmitoylphosphatidylcholine and palmitic acid. Correlations between structural rearrangements, specific volume changes and endothermic events. *Chem. Phys. Lipids.* 48L:205–214.

Koynova, R., B. Tenchov, and G. Rapp. 1997b. Mixing behavior of saturated short-chain phosphatidylcholines and fatty acids. Eutectic points, liquid and solid phase immiscibility, non-lamellar phases. *Chem. Phys. Lipids.* 88:45–61.

Landh, T. 1995. From entangled membranes to eclectic morphologies: cubic membranes as subcellular space organizers. *FEBS Lett.* 369: 13–17.

Larsson, K. 1988. Anesthetic effect and a lipid bilayer transition involving periodic curvature. *Langmuir.* 4:215–217.

Larsson, K. 1989. Cubic lipid-water phases: structure and biomembrane aspects. *J. Phys. Chem.* 93:7304–7314.

Lindblom, G., and L. Rilfors. 1989. Cubic structures and isotropic structures formed by membrane lipids—possible biological relevance. *Biochim. Biophys. Acta.* 988:221–256.

Lindblom, G., and L. Rilfors. 1990. Structures formed by membrane lipids—physicochemical properties and possible biological relevance for membrane function. *In* Dynamics and Biogenesis of Membranes. J. A. F.

Op den Kamp, editor. NATO ASI Series, Vol. H 40. Springer-Verlag, Berlin and Heidelberg. 43–64.

Luzzati, V. 1968. X-ray diffraction studies of lipid-water systems. *In* Biological Membranes, Physical Fact and Function. D. Chapman, editor. Academic Press, New York. 71–123.

Luzzati, V. 1997. Biological significance of lipid polymorphism: the cubic phases. Commentary. *Curr. Opin. Struct. Biol.* 7:661–668.

Luzzati, V., H. Delacroix, and A. Gulik. 1996. The micellar cubic phase of lipid-containing systems: analogies with foams, relations with the infinite periodic minimal surfaces, sharpness of the polar/apolar partition. *J. Phys. II France.* 6:405–418.

Luzzati, V., H. Delacroix, A. Gulik, T. Gulik-Krzywicki, P. Mariani, and R. Vargas. 1997. The cubic phases of lipids. *In* Lipid Polymorphism and Membrane Properties. R. M. Epand, editor. Academic Press, San Diego. 3–24.

Luzzati, V., R. Vargas, P. Mariani, A. Gulik, and H. Delacroix. 1993. Cubic phases of lipid-containing systems. Elements of a theory and biological connotations. *J. Mol. Biol.* 229:540–551.

Mackay, A. L. 1985. Periodic minimal surfaces. *Physica.* 131B:300–305.

Madin, K. A. C., and J. H. Crowe. 1975. Anhydrobiosys in nematodes: carbohydrate and lipid metabolism during dehydration. *J. Exp. Zool.* 211:335–342.

Mariani, P., V. Luzzati, and H. Delacroix. 1988. Cubic phases of lipid-containing systems: structure analysis and biological implications. *J. Mol. Biol.* 204:165–189.

Rapp, G., A. Gabriel, M. Dosiere, and M. H. J. Koch. 1995. A dual detector single readout system for simultaneous small- (SAXS) and wide-angle (WAXS) scattering. *Nuclear Instrum. Methods Phys. Res. A.* 357: 178–182.

Rapp, G., and R. S. Goody. 1991. Light as a trigger for time-resolved structural experiments on muscle, lipids, p21 and bacteriorhodopsin. *J. Appl. Crystallogr.* 24:857–865.

Rappolt, M., and G. Rapp. 1996. Simultaneous small- and wide-angle x-ray diffraction during the main transition of dimyristoylphosphatidylethanolaimine. *Ber. Bunsenges. Phys. Chem.* 100:1153–1162.

Rietveld, A. G., M. C. Koorengevel, and B. De Kruijff. 1995. Non-bilayer lipids are required for efficient protein transport across the plasma membrane of *Escherichia coli. EMBO J.* 14:5506–5513.

Sadoc, J. F., and J. Charvolin. 1989. Infinite periodic minimal surfaces and their crysallography in the hyperbolic plane. *Acta Crystallogr. A.* 45: 10–20.

Seddon, J. 1990. Structure of the inverted hexagonal (H_{II}) phase and non-lamellar phase transitions of lipids. *Biochim. Biophys. Acta.* 1031: 1–69.

Seddon, J., G. Cevc, and D. Marsh. 1983. Calorimetric studies of the gel-fluid (L_β-L_α) and lamellar-inverted hexagonal (L_α-H_{II}) phase transitions in dialkyl- and diacylphosphatidylethanolamines. *Biochemistry.* 22:1280–1289.

Seddon, J. M., J. L. Hogan, N. A. Warrender, and E. Pebay-Peyroula. 1990. Structural studies of phopsholipid cubic phases. *Prog. Colloid Polym. Sci.* 81:189–197.

Seddon, J. M., and R. H. Templer. 1993. Cubic phases of self-assembled amphiphilic aggregates. *Philos. Trans. R. Soc. Lond. A.* 344:377–401.

Seddon, J. M., and R. H. Templer. 1995. Polymorphism of lipid-water systems. *In* Handbook of Biological Physics. R. Lipowsky and E. Sackmann, editors. Elsevier Science, Amsterdam. 97–160.

Shyamsunder, E., S. M. Gruner, M. W. Tate, D. C. Turner, P. T. C. So, and C. P. S. Tilcock. 1988. Observation of inverted cubic phase in hydrated dioleoylphosphatidylethanolamine membranes. *Biochemistry.* 27: 2332–2336.

Siegel, D.P. 1986a. Inverted micellar intermediates and the transitions between lamellar, cubic, and inverted hexagonal lipid phases. 1. Mechanism of the L_α-H_{II} phase transitions. *Biophys. J.* 49:1155–1170.

Siegel, D. P. 1986b. Inverted micellar intermediates and the transitions between lamellar, cubic, and inverted hexagonal lipid phases. 2. Implications for membrane-membrane interactions and membrane fusion. *Biophys. J.* 49:1171–1183.

Siegel, D. P. 1986c. Inverted micellar intermediates and the transitions between lamellar, cubic and inverted hexagonal amphiphile phases. *Chem. Phys. Lipids.* 42:279–301.

Siegel, D. P., and J. L. Banschbach. 1990. Lamellar/inverted cubic (L_α/Q_{II}) phase transitions in N-methylated dioleoylphosphatidylethanolamine. *Biochemistry.* 29:5975–5981.

Templer, R. H., J. M. Seddon, and N. A. Warrender. 1994. Measuring the elastic parameters for inverse bicontinuous cubic phases. *Biophys. Chem.* 49:1–12.

Templer, R. H., D. C. Turner, P. Harper, and J. M. Seddon. 1995. Corrections to some models of the curvature elastic energy of inverse bicontinuous cubic phases. *J. Phys. II. France.* 5:1053–1065.

Tenchov, B., M. Rappolt, R. Koynova, and G. Rapp. 1996. New phases induced by sucrose in saturated phosphatidylethanolamines: an expanded lamellar gel phase and a cubic phase. *Biochim. Biophys. Acta.* 1285:109–122.

Veiro, J. A., R. G. Khalifah, and E. S. Rowe. 1990. ^{31}P nuclear magnetic resonance studies of the appearance of an isotropic component in dielaidoylphosphatidylethanolamine. *Biophys. J.* 57:637–641.